



# Heat capacity measurement of $(\text{Cr}_{1-x}\text{Fe}_x)_3\text{Te}_4$ ( $x = 0-0.1$ ) at high temperatures

Katsuhiro Yasui, Kazushige Ishida<sup>1</sup>, Toshihide Tsuji<sup>\*</sup>

*Department of Nuclear Engineering, Faculty of Engineering, Nagoya University, Furo-cho, Chikusa-ku, Nagoya 464-01, Japan*

## Abstract

Heat capacities of  $(\text{Cr}_{1-x}\text{Fe}_x)_3\text{Te}_4$  ( $x = 0, 0.02, 0.04$  and  $0.1$ ) were measured from 325 to 920 K by using an adiabatic scanning calorimeter. The sample of  $x = 0.1$  showed two heat capacity anomalies. For  $x = 0, 0.02$  and  $0.04$ , heat capacity anomalies were observed at 904, 900 and 890 K, respectively, presumably due to the order–disorder of chromium atoms and vacancies in  $(\text{Cr}_{1-x}\text{Fe}_x)_3\text{Te}_4$ . The transition enthalpy and entropy due to the order–disorder of chromium atoms and vacancies were determined from excess heat capacities. It was found that transition temperatures, enthalpies and entropies decreased with increasing iron contents, indicating that some of the nearest neighbor chromium vacancies neighboring iron sites may not contribute to the order–disorder transition. From the heat capacity, it was found that the solubility limit of iron to  $\text{Cr}_3\text{Te}_4$  was between  $x = 0.04$  and  $0.1$ . © 1997 Elsevier Science B.V.

## 1. Introduction

Tellurium is a corrosive element having a fission yield of about 1% in fast breeder reactors and may attack the inner surface of fuel cladding made of stainless steel, in the presence of oxygen, cesium, iodine, etc. [1,2]. The presence of tellurium in the gap between cladding and fuel has been reported by some investigators [3,4]. For the evaluation of the reaction between stainless steel cladding and fission product tellurium, the thermodynamic data in the iron–chromium–tellurium system are necessary. Heat capacity data are available for binary iron- and chromium-tellurides, but are lacking for ternary iron–chromium-telluride.

In the chromium–tellurium system, there exist some compounds having nickel-arsenide type structure, where chromium atoms are missing in every second layer as seen in Fig. 1 [5]. For the stoichiometric  $\text{Cr}_3\text{Te}_4$ , an order–dis-

order transition which connects with disordering of chromium vacancies has been observed by Grønvd [6]. Moreover, it is known from magnetic susceptibility that iron is soluble up to 8% in  $\text{Cr}_3\text{Te}_4$  [7]. In this study, the heat capacities of  $(\text{Cr}_{1-x}\text{Fe}_x)_3\text{Te}_4$  ( $x = 0, 0.02, 0.04$  and  $0.1$ ) were measured in the temperature range from 325 to 920 K by an adiabatic scanning calorimeter to know how the thermodynamic data change with increasing iron contents and to know solubility limit of iron to  $\text{Cr}_3\text{Te}_4$ .

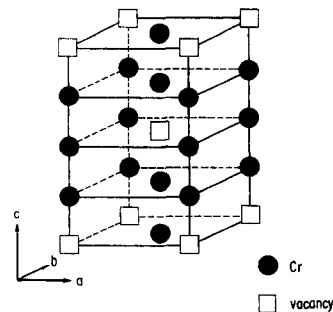


Fig. 1. Unit cell of  $\text{Cr}_3\text{Te}_4$ . In the figure, Te atoms are omitted for clarity.

<sup>\*</sup> Corresponding author. Tel.: +81-52 789 3776; fax: +81-52 789 4685; e-mail: t-tsuji@nucl.nagoya-u.ac.jp.

<sup>1</sup> Present address: Energy Research Laboratory, Hitachi, Ltd., 1168 Moriyama-cho, Hitachi-shi, Ibaraki-ken, 316 Japan.

## 2. Experimental

### 2.1. Sample preparation

The starting materials used for sample preparation were high-purity chromium (99.99%), iron (99.99%) and tellurium (99.999%). The parts of  $(\text{Cr}_{1-x}\text{Fe}_x)_3\text{Te}_4$  ( $x = 0, 0.02, 0.04$  and  $0.1$ ) samples prepared in our laboratory for magnetic susceptibility measurements [7] were used for heat capacity measurements in this study, and details of the sample preparation have been described elsewhere [7,8]. The chromium, iron and tellurium having the desired concentration were mixed and put into a silica capsule which was then evacuated and finally sealed under vacuum. The sample was heated to 1273 K over a period of 7 days, kept at this temperature for 2 days, annealed at 1073 K for 2 days, and cooled to room temperature. The sample obtained was finely crushed and sealed in another silica capsule. The sealed sample was heated to 1073 K over a period of 2 days and kept at this temperature for 5 days. This sample was slowly cooled to 673 K, kept at this temperature for 10 days and then slowly cooled to room temperature.

For  $x = 0, 0.02$  and  $0.04$ , X-ray powder diffraction patterns showed the existence of a single phase with monoclinic structure, whereas the sample for  $x = 0.1$  was a phase with NiAs-type crystal structure [7]. The lattice parameters of  $\text{Cr}_3\text{Te}_4$  used for this experiment was described in Ref. [7] and were in good agreement with those reported by Grønvold [6].

### 2.2. Heat capacity measurement

Heat capacities of  $(\text{Cr}_{1-x}\text{Fe}_x)_3\text{Te}_4$  ( $x = 0, 0.02, 0.04$  and  $0.1$ ) were measured in the temperature range of 325–

920 K by using an adiabatic scanning calorimeter [9]; in this calorimeter the power supplied to the sample was measured continuously, and the heating rate was kept constant regardless of the type and amount of the sample. The heating rate chosen was  $2 \text{ K min}^{-1}$ , and the measurement was carried out between 325 and 920 K under a pressure of about 130 Pa of air by using the sample of 16–20 g sealed in a quartz vessel filled with helium gas at 20 kPa. The heating rate and adiabatic control were usually maintained within  $\pm 0.005 \text{ K min}^{-1}$  and  $\pm 0.01 \text{ K}$ , respectively. The heat capacity measurement was conducted within an imprecision of  $\pm 3\%$  and an inaccuracy of  $\pm 2\%$ .

## 3. Results and discussion

### 3.1. Heat capacity of $(\text{Cr}_{1-x}\text{Fe}_x)_3\text{Te}_4$ ( $x = 0, 0.02, 0.04$ and $0.1$ )

The results of heat capacity measurements of  $(\text{Cr}_{1-x}\text{Fe}_x)_3\text{Te}_4$  ( $x = 0, 0.02, 0.04$  and  $0.1$ ) are shown in Fig. 2(a)–(d). Heat capacity anomalies are observed at 904, 900 and 890 K for  $x = 0, 0.02$  and  $0.04$  in monoclinic  $(\text{Cr}_{1-x}\text{Fe}_x)_3\text{Te}_4$ , respectively, presumably due to the order–disorder of chromium atoms and vacancies in  $(\text{Cr}_{1-x}\text{Fe}_x)_3\text{Te}_4$ . However, for  $x = 0.1$  having NiAs type crystal structure, a large heat capacity anomaly is seen at 706 K in Fig. 2(d), presumably due to the order–disorder transition of chromium atoms and vacancies. A small peak at 780 K is probably the order–disorder transition in monoclinic phase which could not be detected by X-ray diffractometry. Therefore, it is probable that the sample of  $x = 0.1$  is two-phase mixture and solubility limit of iron to  $\text{Cr}_3\text{Te}_4$  lies between  $x = 0.04$  and  $x = 0.1$ . Small heat capacity anomalies seen near room temperature in Fig.

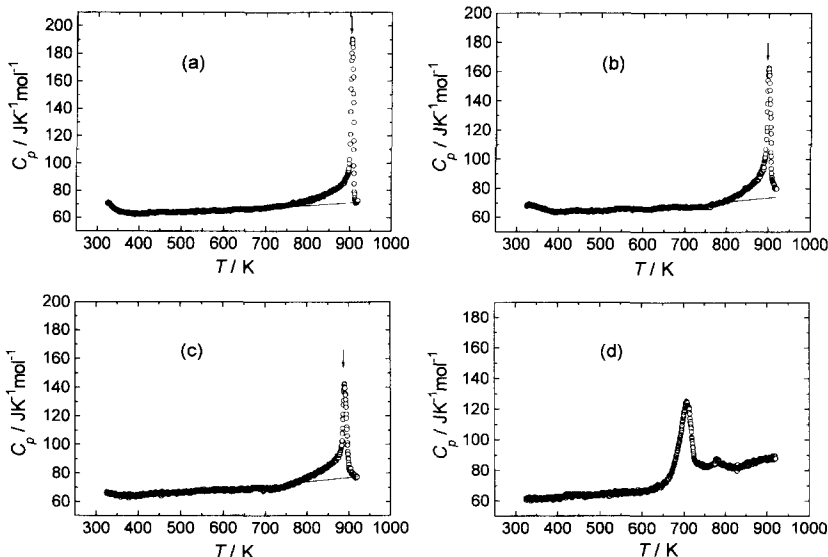


Fig. 2. Heat capacities of  $(\text{Cr}_{1-x}\text{Fe}_x)_3\text{Te}_4$  as a function of temperature. (a)  $x = 0$  (b)  $x = 0.02$  (c)  $x = 0.04$  and (d)  $x = 0.1$ .

Table 1

Transition temperature ( $T_{tr}$ ), transition enthalpy ( $\Delta H_{tr}$ ) and entropy ( $\Delta S_{tr}$ ) changes for  $(Cr_{1-x}Fe_x)Te_{1.33}$  i.e.,  $(Cr_{1-x}Fe_x)_3Te_4$

$x$	$T_{tr}$ (K)	$\Delta H_{tr}$ (kJ mol <sup>-1</sup> )	$\Delta S_{tr}$ (J K <sup>-1</sup> mol <sup>-1</sup> )	References
0	903	2.28	2.52	Grønvoid [6]
0	904	2.00	2.29	this work
0.02	900	1.78	2.01	this work
0.04	890	1.55	1.78	this work

2(a)–(c) correspond to ferro- to para-magnetic transition measured by magnetic susceptibility [7] which will be described later. In Fig. 2(d), the increase of heat capacity over 820 K may be caused by the activation process such as defect formation, electron excitation or electron–hole pair formation observed for  $Ni_5Te_8$  in our previous study [10].

In order to estimate the transition enthalpy and entropy changes, it is necessary to get the base line of heat capacity,  $C_p$ . The base line was determined by the least square method as follows:

$$C_p(T) = A + BT + C/T^2, \quad (1)$$

where  $T$  is the absolute temperature and  $A$  to  $C$  are the coefficients of polynomial terms in Eq. (1). As seen in Fig. 2(a)–(c), the order–disorder transition temperatures decrease and the shapes of their peaks become broader with increasing the iron contents. The order–disorder phase transition for  $x = 0$  is considered to be finished because of a sharp peak, although the transition temperature of this composition is higher than those of other ones. On the other hand, for  $x = 0.04$  the phase transition temperature can be low enough to obtain the transition enthalpy and entropy changes from heat capacity data in spite of the broader peak. For the sample of  $x = 0.02$  having the intermediate transition temperature and the intermediate broadness of the peak, phase transition does not seem to be finished even at 920 K which is the measuring upper limit of our adiabatic scanning calorimeter. For the calculation of the base line, Eq. (1) was applied to heat capacity data in the temperature ranges of 400–600 K and 915–920 K for both  $x = 0$  and  $x = 0.04$  samples and that of 400–600 K for  $x = 0.02$ . The base lines obtained in this study are shown in Fig. 2(a)–(c). For  $x = 0.02$ , transition enthalpy and entropy were calculated by extrapolating heat capacity data to higher temperature. The transition temperature, transition enthalpy and entropy changes obtained in this study are shown in Table 1. For  $x = 0$ , transition temperature in this study agrees well with that measured by Grønvoid [6]. Transition enthalpy and entropy obtained in this study are also close to that evaluated by him. As seen in the table, transition temperatures, transition enthalpies and entropies decrease with increasing iron contents.

Grønvoid [6] calculated theoretically the transition entropy ( $3.84 \text{ J K}^{-1} \text{ mol}^{-1}$ ) for  $CrTe_{1.33}$ , i.e.,  $Cr_3Te_4$  on the

assumption that the order–disorder of chromium atoms and vacancies occurs only within the layers in which vacancies locate, as follows (see Fig. 1):

$$\text{For } CrTe_{1.33} = (2/3)\{CrTe(Cr_{1/2} \square_{1/2})Te\}$$

$$\Delta S_{tr} = (2/3)k \ln({}_N C_{N/2}) = (2/3)R \ln 2$$

$$= 3.84 \text{ J K}^{-1} \text{ mol}^{-1},$$

where  $k$  is the Boltzmann's constant,  $N$  is the Avogadro's constant,  $R$  is the gas constant and  $\square$  is the chromium vacancy. Both the experimental values obtained in this study and by Grønvoid are smaller than the theoretical one. This fact suggests that the completely-ordered phase at low temperatures is not formed even in the slowly cooled sample or that the partially-ordered phase still remains even at high temperatures at which measurements were made. Considering the ratio of order–disorder transition temperature (about 900 K) to the melting point (about 1500 K) for  $Cr_3Te_4$ , the former possibility is higher than the latter one. Since the solubility limit of iron to  $Cr_3Te_4$  is small and all the samples were made by the same thermal history, it is thus considered that the doped iron atoms affect at least the neighboring chromium atoms and vacancies, and do not influence to the partially-ordered state of chromium atoms and vacancies apart from the doped iron atoms.

Let us consider two models for the effect of iron on the order–disorder phase transition of  $(Cr_{1-x}Fe_x)_3Te_4$ . In the model 1, the order–disorder transition entropy was calculated on the assumption that iron substitutes randomly for chromium in the layers containing vacancy and iron atoms are independent of the order–disorder transition, as follows.

$$\text{For } Cr_{1-x}Fe_xTe_{1.33} = (2/3)[CrTe(Cr_{(1/2)-(3x/2)}Fe_{3x/2}\square_{1/2})Te],$$

$$\begin{aligned} \Delta S_{tr} &= (2/3)k \ln({}_{(1-(3x/2))N} C_{N/2}) \\ &= (2/3)R \{ [1 - (3x/2)] \ln \{ 1 - (3x/2) \} \\ &\quad - \{ (1/2) - (3x/2) \} \ln \{ (1/2) - (3x/2) \} \\ &\quad - (1/2) \ln(1/2) \}. \end{aligned} \quad (2)$$

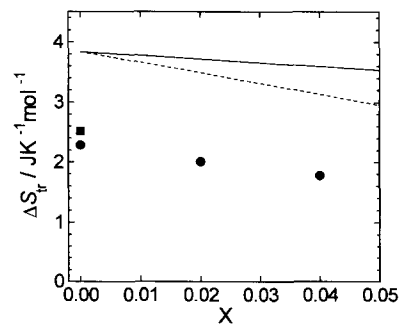


Fig. 3. Transition entropy changes for  $(Cr_{1-x}Fe_x)Te_{1.33}$ . This work (●), Grønvoid (■), model 1 (—) and model 2 (---).

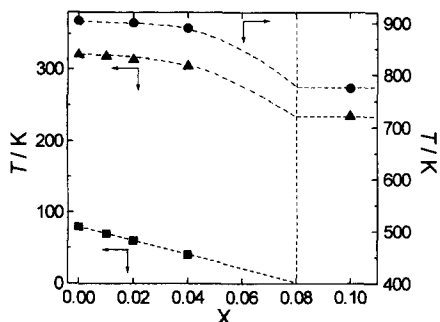


Fig. 4. Variation of magnetic transition temperatures and order-disorder transition temperatures for  $(\text{Cr}_{1-x}\text{Fe}_x)_3\text{Te}_4$  against the  $x$  value. Antiferro- to ferro-magnetic transition (■), ferro- to para-magnetic transition (▲) [7] and order-disorder transition (●).

In the model 2, transition entropy is calculated on the assumption that the iron substitutes randomly for chromium in the layers containing vacancy and the chromium vacancies neighboring iron sites in addition to iron atoms are independent of the order-disorder transition, and is expressed by the following equation:

For  $\text{Cr}_{1-x}\text{Fe}_x\text{Te}_{1.33} = 2/3[\text{CrTe}(\text{Cr}_{(1/2)-(3x/2)}\square_{(1/2)-3x}(\text{Fe}_{3x/2}\square_{3x})\text{Te})]$ ,

$$\begin{aligned} \Delta S_{\text{tr}} &= 2/3k \ln \left( {}_{\{1-(9x/2)\}N} C_{\{(1/2)-3x\}N} \right) \\ &= 2/3R \left[ \{1-(9x/2)\} \ln \{1-(9x/2)\} \right. \\ &\quad \left. - \{(1/2)-3x\} \ln \{(1/2)-3x\} \right. \\ &\quad \left. - \{(1/2)-(3x/2)\} \ln \{(1/2)-(3x/2)\} \right]. \quad (3) \end{aligned}$$

The theoretical values for two models, together with the experimental values are shown in Fig. 3 as a function of  $x$ . The slope of the experimental values lies between models 1 and 2. It is thus considered that some of the chromium

vacancies neighboring iron sites may be independent of the order-disorder transition.

### 3.2. Solubility limit of iron to $\text{Cr}_3\text{Te}_4$

The magnetic properties of  $(\text{Cr}_{1-x}\text{Fe}_x)_3\text{Te}_4$  have been measured by Hinatsu et al. [7]. In Fig. 4, the antiferro- to ferro-magnetic transition temperature (Néel point) and ferro- to para-magnetic transition (Curie point) are plotted against the iron contents, together with the order-disorder transition temperature measured in this study. The solubility limit of iron has been determined to be about  $x = 0.08$  by using Néel temperatures against  $x$  by Hinatsu et al. [7]. It is found from heat capacity measurement that solubility limit of iron to  $\text{Cr}_3\text{Te}_4$  lies between  $x = 0.04$  and  $x = 0.1$  which is consistent with the solubility limit determined by magnetic susceptibility.

### References

- [1] M.G. Adamson, E.A. Aitken, Proc. Int. Conf. on Fast Breeder Reactor Fuel Performance, Monterey, CA, 1979, p. 536.
- [2] M.G. Adamson, E.A. Aitken, T.B. Lindermer, J. Nucl. Mater. 130 (1985) 375.
- [3] J.W. Weber, E.D. Jensen, Trans. Am. Nucl. Soc. 14 (1971) 175.
- [4] C.T. Walker, J. Nucl. Mater. 74 (1978) 358.
- [5] M. Chevreton, F. Bertaut, Comptes Rendus (Paris) 253 (1961) 145.
- [6] F. Grønvald, J. Chem. Thermodyn. 5 (1973) 545.
- [7] Y. Hinatsu, K. Ishida, T. Tsuji, J. Solid-State Chem. 120 (1995) 49.
- [8] T. Tsuji, T. Kato, K. Naito, J. Nucl. Mater. 201 (1993) 120.
- [9] K. Naito, H. Inaba, M. Ishida, Y. Saito, H. Arima, J. Phys. E7 (1974) 464.
- [10] T. Tsuji, K. Ishida, Thermochem. Acta 253 (1995) 11.